Journal of Solid Mechanics Vol. 11, No. 3 (2019) pp. 644-656
DOI: 10.22034/JSM.2019.666692

Buckling Analysis of Functionally Graded Shallow Spherical Shells Under External Hydrostatic Pressure

M. Hosseini *, F. Karami

Mechanical Engineering Department, Faculty of Engineering, Malayer University, Malayer, Iran

Received 23 June 2019; accepted 25 August 2019

ABSTRACT

The aim of this paper is to determine the critical buckling load for simply supported thin shallow spherical shells made of functionally graded material (FGM) subjected to uniform external pressure. A metal-ceramic functionally graded (FG) shell with a power law distribution for volume fraction is considered, where its properties vary gradually through the shell thickness direction from pure metal on the inner surface to pure ceramic on the outer surface. First, the total potential energy functional is obtained using the first-order shell theory of Love and Kirchhoff, Donnell-Mushtari-Vlasov kinematic equations and Hooke's Law. Then, equilibrium equations are derived through the minimization of the total potential energy functional by employing the Euler equations. The stability equations are derived by application of the adjacent - equilibrium criterion. As the nonlinear strain-displacement relations are employed, so the presented analysis is nonlinear with high accuracy. The Galerkin method is used to determine the critical buckling load. The present problem is also analyzed numerically by simulating it in Abaqus software. For validation, the present analytical results are compared with the present numerical results and with the known data in the literature. Also, the effects of some important geometrical and mechanical parameters on the hydrostatic buckling pressure are investigated.

Keywords: Buckling; Spherical shell; FGM; External hydrostatic pressure.

1 INTRODUCTION

IN recent years, with the increasing and rapid development of various industries, the advancements in industrial machinery and the developments in high-powered engines of aerospace industry, turbines and reactors and other machinery, the need for mechanically stronger materials with higher thermal resistance has been felt. In previous years, pure ceramic materials were used in the aerospace industry for the coating of the components with high

*Corresponding author. Tel.: +98 813 2233114.
E-mail address: m.hosseini27@gmail.com (M.Hosseini).

performance. These materials were very good non-conductors but were not resistant enough to residual stress. Residual stresses caused many problems such as cavities and cracks in these materials. Layered composites were used later to overcome this problem. Thermal stresses also made them chip. Regarding these problems, producing a composite material which has high thermal and mechanical resistance and is immune to chipping gained in importance.

In 1939, Von karman and Tsien [1] analytically investigated the buckling of spherical shells subjected to external pressure. They derived the governing equations of the system through minimizing the total potential energy. Then obtained approximate solution using the Rayleigh-Ritz method. In 1987, Wahhaj Uddin [2] studied the stability of general spherical shells under external pressure with various end-conditions. The governing nonlinear differential equations for the axisymmetric deformations of spherical shells, were solved exactly by using the method of multisegment integration. Numerical results for a few shells, ranging from shallow to hemispherical, were presented as examples and compared with the available works of others. In 2000, Zang et al. [3] investigated dynamic non-linear axisymmetric buckling of laminated cylindrically orthotropic composite shallow spherical shells including third-order transverse shear deformation. In 2001, Nie [4] formulated an asymptotic solution for non-linear buckling of elastically restrained imperfect shallow spherical shells continuously supported on a non-linear elastic foundation.

In 2003, Li et al. [5] established the large deflection equation of a shallow spherical shell under uniformly distributed transverse loads is with consideration of effects of transverse shear deformation on flexural deformation. In 2008, Gupta et al.[6] conducted experiments, simulation as well as analysis of the collapse behavior of thin spherical shells under quasi-static loading. In 2008, Sorensen and Jensen [7] carried out an analysis of buckling-driven delamination of a layer in a spherical, layered shell. In 2010, Hutchinson [8] revealed that cylindrical shells under uniaxial compression and spherical shells under equi-biaxial compression display the most extreme buckling sensitivity to imperfections.

In 2010, Darvizeh et al. [9] investigated the thermal buckling of composite shells with selected boundary conditions under uniform and linearly distributed thermal load. The theoretical modeling procedure was based on semi-analytical finite element method. The effects of important structural parameters such as amount of cut-out at apex, fiber angles as well as temperature distributions were taken into consideration. In 2011, Shaterzadeh et al. [10] investigated the thermal post-buckling of shells of revolution under the action of uniform thermal load. They also considered the effect of initial imperfection. The semi-analytical finite element method was employed to discretize the problem. Then, the nonlinear equations were solved by means of the Newton-Raphson algorithm in conjunction with the Arc length method. In 2012, Sato et al. [11] studied the critical buckling characteristics of hydrostatically pressurized complete spherical shells filled with an elastic medium. In 2014, Boroujerdy and Eslami [12] studied the snap-through buckling of shallow clamped spherical shells made of functionally graded material and surface-bonded piezoelectric actuators under the thermo-electro-mechanical loading.

2 FORMULATIONS

The considered FGM shallow spherical shell is made of metal and ceramics, so that its properties gradually vary from pure ceramics at the outer surface to pure metal at the inner surface (Fig. 1).

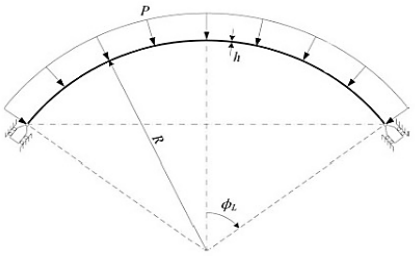

Fig.1
A schematic view of the FGM shallow spherical shell. [13]

Voigt notation is used for elastic modulus, but Poisson's ratio is assumed to be constant. The mechanical properties variations are assumed to be [14]:

$$E(z) = E_c V_c + E_m V_m$$
$$\nu(z) = \nu \tag{1}$$

where V_m and V_c are the volume fraction of metal and ceramics which are defined as follows[4]:

$$V_m = (z/h + 1/2)^k$$
$$V_c = 1 - V_m \tag{2}$$

In Eqs. (1) and (2), the coordinate z is measured from the middle surface of the shell which varies from $-h/2$ to $h/2$. The positive direction of z outwards. For the spherical geometry of the considered shell φ, θ and z are meridional, circumferential and radial directions respectively which create an orthogonal coordinate system. Subscripts m and c stand for metal and ceramic respectively. The parameter k is the power law index for the volume fraction for which values greater than or equal to zero can be considered. Substituting Eq. (2) in Eq. (1) gives:

$$E(z) = E_m + E_{cm}\left(\frac{2z+h}{2h}\right)^k$$
$$\nu(z) = \nu \tag{3}$$

where

$$E_{cm} = E_c - E_m \tag{4}$$

According to the first-order shell theory of Love and Kirchhoff, the normal and shear strains at the distance z from the middle surface of the shell are [15]:

$$\varepsilon_\varphi = \varepsilon_{\varphi m} + zk_\varphi$$
$$\varepsilon_\theta = \varepsilon_{\theta m} + zk_\theta \tag{5}$$
$$\gamma_{\varphi\theta} = \gamma_{\varphi\theta m} + 2zk_{\varphi\theta}$$

where ε_i and γ_{ij} are the normal and shear strains respectively, k_θ and k_φ are the middle surface bending curvatures, $k_{\varphi\theta}$ is the middle surface twisting curvature, and the subscript m indicates the middle surface.

Through the nonlinear kinematics relations, the strains and bending of the middle surface are related to the displacement components u, v, and w. Sanders nonlinear kinematics relations for thin spherical shell are presented in reference [15]. According to the theory of shallow spherical shells, the DMV nonlinear relations for spherical shell are as the simplified form of Eqs. (6):

$$\varepsilon_{\varphi m} = \frac{u_{,\varphi} + w}{R} + \frac{\beta_\varphi^2}{2}$$
$$\varepsilon_{\theta m} = \frac{v_{,\theta} + u\cos\varphi + w\sin\varphi}{R\sin\varphi} + \frac{\beta_\theta^2}{2}$$
$$\gamma_{\varphi\theta m} = \frac{u_{,\theta} + v_{,\varphi}\sin\varphi - v\cos\varphi}{R\sin\varphi} + \beta_\varphi\beta_\varphi$$
$$k_\varphi = -\frac{w_{,\varphi\varphi}}{R^2} \tag{6}$$
$$k_\theta = -\frac{w_{,\theta\theta}}{R^2\sin\varphi} - \frac{w_{,\varphi}\cot\varphi}{R^2}$$
$$k_{\varphi\theta} = \frac{w_{,\theta}\cot\varphi - w_{,\varphi\theta}}{R^2\sin\varphi}$$

where β_φ and β_θ are the rotations of the normal vector of the middle surface about the θ and φ axes respectively, and:

$$\beta_{\varphi} = -\frac{w_{,\varphi}}{R}$$
$$\beta_{\theta} = -\frac{w_{\theta}}{R\sin\varphi} \tag{7}$$

In Fig. 2 are shown the stresses in a segment of the spherical shell. According to the theory of shallow shells, the effects of the transverse shear stresses $\tau_{\varphi z}$ and $\tau_{\theta z}$ are neglected.

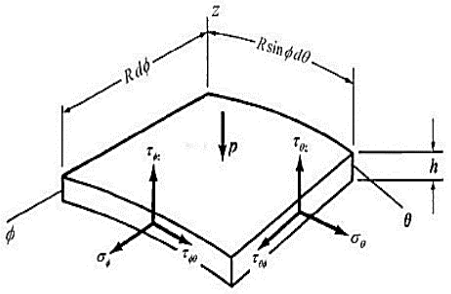

Fig.2
A view of the stresses in a segment of the spherical shell. [16]

Based on the Hooke's Law, the stress-strain relations for spherical shells are as follows [17]:

$$\sigma_{\varphi} = \frac{E(z)}{1-\nu^2}\left(\varepsilon_{\varphi} + \nu\varepsilon_{\theta}\right)$$
$$\sigma_{\theta} = \frac{E(z)}{1-\nu^2}\left(\varepsilon_{\theta} + \nu\varepsilon_{\varphi}\right) \tag{8}$$
$$\tau_{\varphi\theta} = G(z)\gamma_{\varphi\theta}$$

Substituting Eq.(5) and the relation $G(z) = \frac{E(z)}{2(1+\nu)}$ in Eq.(8) yields:

$$\sigma_{\varphi} = \frac{E(z)}{1-\nu^2}\left(\varepsilon_{\varphi m} + \nu\varepsilon_{\theta} + zk_{\varphi} + \nu zk_{\theta}\right)$$
$$\sigma_{\theta} = \frac{E(z)}{1-\nu^2}\left(\varepsilon_{\theta m} + \nu\varepsilon_{\varphi m} + zk_{\theta} + \nu zk_{\varphi}\right) \tag{9}$$
$$\tau_{\varphi\theta} = \frac{E(z)}{2(1+\nu)}\left(\gamma_{\varphi\theta m} + 2zk_{\varphi\theta}\right)$$

According to the theory of shallow shells, the effects of the transverse shear forces $Q_{\varphi z}$ and $Q_{\theta z}$ are ignored. The force resultants N_{ij} and moment resultants M_{ij} are defined in terms of the stresses through the following equations [18]:

$$N_{ij} = \int_{-h/2}^{h/2}\sigma_{ij}dz$$
$$M_{ij} = \int_{-h/2}^{h/2}\sigma_{ij}zdz \tag{10}$$

Substituting Eqs.(9) in Eqs. (10) and calculating the integrals, the force and the moment resultants are obtained as functions of strains and curvatures. In general, the total potential energy V of a loaded body is the sum of the strain energy U and the potential energy of the applied loads Ω [18]:

$$V = U + \Omega \tag{11}$$

Generally, the strain energy U of a three-dimensional body with an arbitrary orthogonal coordinates *x, y* and *z* is as follows [18]:

$$U = \frac{1}{2}\iiint \left(\sigma_x \varepsilon_x + \sigma_y \varepsilon_y + \sigma_z \varepsilon_z + \tau_{xy}\gamma_{xy} + \tau_{yz}\gamma_{yz} + \tau_{zx}\gamma_{zx}\right) dxdydz \tag{12}$$

Noting that the shallow spherical shells have plane stress and plane strain states, so the strain energy U can be written as:

$$U = \frac{1}{2}\iiint \left(\sigma_\varphi \varepsilon_\varphi + \sigma_\theta \varepsilon_\theta + \tau_{\varphi\theta}\gamma_{\varphi\theta}\right) ds_\varphi ds_\theta dz \tag{13}$$

ds_φ and ds_θ are the differential of the arc length about the θ and φ axes respectively which are:

$$\begin{aligned} ds_\varphi &= A\, d\varphi \\ ds_\theta &= B d\theta \end{aligned} \tag{14}$$

where A and B are the Lame parameters whose values for a spherical shell are $A = R$ and $B = R\sin\varphi$. Substituting these values in Eq. (14) gives:

$$\begin{aligned} ds_\varphi &= R d\varphi \\ ds_\theta &= R\sin\varphi d\theta \end{aligned} \tag{15}$$

Substituting the Love-Kirchhoff Eqs. (5), stress-strains Equations of the middle surface (8) and the differential of arc length (15) in the strain energy Eq. (13) and then substituting the mechanical properties of the FGM given in Eqs. (3) and the DMV kinematic relations given in Eqs. (6) in the resultant equation and calculating the integral with respect to coordinate *z*, yields:

$$U = \iint D\left(\varphi,\theta,u,v,w,u_{,\varphi},,u_{,\theta},v_{,\varphi},v_{,\theta},w_{,\varphi},w_{,\theta},w_{,\varphi\varphi},w_{,\theta\theta},w_{,\varphi\theta}\right) d\varphi d\theta \tag{16}$$

Generally, the potential energy Ω of the applied loads for a shell with arbitrary orthogonal coordinates of *x, y* and *z* which is under three-dimensional pressure of P_x, P_y, P_z at all its surfaces, is equal to a negative times of the work done due to this pressure as the following:

$$\Omega = -\iint \left(P_x u + P_y v + P_z w\right) ds_x ds_y \tag{17}$$

Since the pressure is only applied in the *z* direction and in a negative way, so using Eq. (15) and (17), the potential energy due to external hydrostatic pressure Ω is obtained as the following:

$$\Omega = \iint PwR^2 \sin\varphi d\varphi d\theta \tag{18}$$

Substituting Eqs. (16) and (18) in Eq. (11) yields the total potential energy for the considered shell as follows:

$$V = \iint F\begin{pmatrix} \varphi,\theta,u,v,w,u_{,\varphi},u_{,\theta},v_{,\varphi},v_{,\theta},w_{,\varphi} \\ ,w_{,\theta},w_{\varphi\varphi},w_{\theta\theta},w_{\varphi\theta} \end{pmatrix} d\varphi d\theta \tag{19}$$

where

$$F = D + PwR^2 \sin\varphi \tag{20}$$

In order to derive the equilibrium equations, according to the principle of the minimum potential energy for static problems, the total potential energy V should be minimized. To do so, its variations δV must be set equal to zero. Based on the concepts of the calculus of variations, for zero total potential energy variations (δV = 0), the corresponding Euler equations should be applied to the function of Eq. (20). Functional Euler equations like Eq. (19) are as follows [4]:

$$\begin{aligned}
&\frac{\partial F}{\partial u}-\frac{\partial}{\partial \varphi}\frac{\partial F}{\partial u_{,\varphi}}-\frac{\partial}{\partial \theta}\frac{\partial F}{\partial u_{,\theta}}=0\\
&\frac{\partial F}{\partial v}-\frac{\partial}{\partial \varphi}\frac{\partial F}{\partial v_{,\varphi}}-\frac{\partial}{\partial \theta}\frac{\partial F}{\partial v_{,\theta}}=0\\
&\frac{\partial F}{\partial w}-\frac{\partial}{\partial \varphi}\frac{\partial F}{\partial w_{,\varphi}}-\frac{\partial}{\partial \theta}\frac{\partial F}{\partial w_{,\theta}}+\frac{\partial^2}{\partial \varphi^2}\frac{\partial F}{\partial w_{,\varphi\varphi}}+\frac{\partial^2}{\partial \theta^2}\frac{\partial F}{\partial w_{,\theta\theta}}+\frac{\partial^2}{\partial \varphi\partial \theta}\frac{\partial F}{\partial w_{,\varphi\theta}}=0
\end{aligned} \tag{21}$$

Substituting Eq. (20) in Euler Eqs. (21) gives nonlinear equilibrium equations for shallow spherical shells under mechanical load. The equilibrium equations for these shells in terms of the force and moment resultants are:

$$\begin{aligned}
&\cos\varphi N_{\theta}-(\sin\varphi N_{\varphi})_{,\varphi}-N_{\varphi\theta,\theta}=0\\
&N_{\theta,\theta}+(\sin\varphi N_{\varphi\theta})_{,\varphi}+\cos\varphi N_{\varphi\theta}=0\\
&(\sin\varphi M_{\varphi})_{,\varphi}+\frac{1}{\sin\varphi}M_{\theta,\theta\theta}-\left[R\sin\varphi(N_{\varphi}\beta_{\varphi}+N_{\varphi\theta}\beta_{\theta})+\cos\varphi M_{\theta}\right]_{,\varphi}+2(M_{\varphi\theta,\varphi\theta}+\cot\varphi M_{\varphi\theta,\theta})\\
&-R\sin\varphi(N_{\varphi}+N_{\theta})-R(N_{\theta}\beta_{\theta}+N_{\varphi\theta}\beta_{\varphi})_{,\theta}=PR^2\sin\varphi
\end{aligned} \tag{22}$$

Based on the the Adjacent-Equilibrium Criterion, to obtain the stability equations, the displacements are given a very small virtual variation [4], so that the displacements of the middle surface in the pre-buckling or equilibrium state, caused by the applied loads (no variation is made in the applied loads), and the displacements of the virtual middle surface are very small. The displacements of the virtual middle surface result in corresponding changes in the force and moment resultants [4], so that the pre-buckling force and moment resultants and the virtual force and moment resultants correspond to the displacements of the virtual middle surface. Substituting the force and moment resultants and β_{φ_0}, β_{φ_1}, β_{θ_0}, β_{θ_1} in the equilibrium Eqs. (22), some of the terms of these equations are removed. The pre-buckling rotation of the vector normal to the middle surface about axis φ (i.e. β_{θ_0}) is zero, due to the symmetry of the applied mechanical load. Also, the effect of the pre-buckling rotation of the vector normal to the middle surface about axis θ (i.e. β_{θ_0}) is neglected. So the equations become as the following simple form:

$$\begin{aligned}
&\cos\varphi N_{\theta_1}-(\sin\varphi N_{\varphi_1})_{,\varphi}-N_{\varphi\theta,\theta}=0\\
&N_{\theta_1,\theta}+(\sin\varphi N_{\varphi\theta_1})_{,\varphi}+\cos\varphi N_{\varphi\theta_1}=0\\
&(\sin\varphi M_{\varphi_1})_{,\varphi\varphi}+\frac{M_{\theta_1,\theta\theta}}{\sin\varphi}\left[R\sin\varphi(N_{\varphi_0}\beta_{\varphi_1}+N_{\varphi\theta_0}\beta_{\theta_1})+\cos\varphi M_{\theta_1}\right]_{,\varphi}+2\left[M_{\varphi\theta_1,\varphi\theta}+\cot\varphi M_{\varphi\theta_1,\theta}\right]\\
&-R\sin\varphi(N_{\varphi_1}+N_{\theta_1})-R(N_{\theta_0}\beta_{\theta_1}+N_{\varphi\theta_0}\beta_{\varphi_1})_{,\theta}=0
\end{aligned} \tag{23}$$

Relations (23) are the stability equations for the shallow spherical shells. As mentioned before, the subscripts 1 and 0 represent the equilibrium and the stability states respectively. In fact, the terms with subscript 0 are obtained by solving the equilibrium equations.

To calculate the pre-buckling force resultants, the membrane solution of the equilibrium equations is considered for the sake of simplicity, in other words, the moment resultants are ignored.

Setting $\beta_{\varphi_0}=\beta_{\theta_0}=0$ and removing the moment resultants expressions, the membrane form of the equilibrium Eqs. (22) is obtained:

$$\begin{aligned}
&\cos\varphi N_{\theta_0} - (\sin\varphi N_{\varphi_0})_{,\varphi} - N_{\varphi\theta_0,\theta} = 0\\
&N_{\theta_0,\theta} + (\sin\varphi N_{\varphi\theta_0})_{,\varphi} + \cos\varphi N_{\varphi\theta_0} = 0\\
&-R\sin\varphi(N_{\varphi_0} + N_{\theta_0}) = PR^2\sin\varphi
\end{aligned} \tag{24}$$

Since the applied hydrostatic pressure is symmetric, so, it can be written that:

$$\begin{aligned}
&N_{\varphi} = N_{\theta}\\
&N_{\varphi\theta_0} = 0
\end{aligned} \tag{25}$$

Regarding that N_{φ_0} and N_{θ_0} are equal, simplifying the sum of the third variation of Eq.(25) yields:

$$N_{\varphi_0} = N_{\theta_0} = -\frac{PR}{2} \tag{26}$$

According to Eq. (25) and Eq. (26) the first and the second variations of Eq. (24) are satisfied. So, the pre-buckling force resultants for a shell subjected to external hydrostatic pressure are as follows:

$$\begin{aligned}
&N_{\varphi_0} = N_{\theta_0} = -\frac{PR}{2}\\
&N_{\varphi\theta_0} = 0
\end{aligned} \tag{27}$$

The simply supported boundary conditions of the problem can be written as the followings:

$$u_{1,\varphi} = v_1 = w_{1,\varphi\varphi} = w_1 = 0 \qquad at \qquad \varphi = \varphi_L \tag{28}$$

The one-term solution to the stability Eqs. (23) which satisfies the assumed boundary conditions is considered as the following [4 and 15]:

$$\begin{aligned}
&u_1 = A_1\cos n\theta\cos\lambda\varphi\\
&v_1 = B_1\sin n\theta\sin\lambda\varphi \qquad 0 \le \varphi \le \varphi_L\\
&w_1 = C_1\cos n\theta\sin\lambda\varphi \qquad 0 \le \theta \le 2\pi
\end{aligned} \tag{29}$$

where $\lambda = m\pi/\varphi_L$ is the angle between the line perpendicular to the spherical shell and the line passing through the border and m=1,2,3,… and n=1,2,3,…are the numbers of the meridional and circumferential waves respectively and A_1, B_1, C_1 are constants.

Substituting the approximate solutions (29) in the stability Eqs. (23) gives a system of equations as follows:

$$\begin{aligned}
&R_{11}A_1 + R_{12}B_1 + R_{13}C_1 = E_1\\
&R_{21}A_1 + R_{22}B_1 + R_{23}C_1 = E_2\\
&R_{31}A_1 + R_{32}B_1 + R_{33}C_1 = E_3
\end{aligned} \tag{30}$$

where R_{ij} are functions of the parameters λ and n, the geometrical parameters h and R, the applied load P, the mechanical properties of the FGM and the independent variables φ and θ. Errors E_1, E_2, E_3 are due to the approximate solutions. The Galerkin method is utilized to minimize these errors. The approximate solutions (30) are substituted in stability Eq. (24). Then, employing Galerkin minimization technique gives:

$$\begin{aligned}
&a_{11}A_1 + a_{12}B_1 + a_{13}C_1 = 0\\
&a_{21}A_1 + a_{22}B_1 + a_{23}C_1 = 0\\
&a_{31}A_1 + a_{32}B_1 + a_{33}C_1 = 0
\end{aligned} \tag{31}$$

For the system of Eq. (31) to have a nontrivial solution, where the buckling occurs, the determinant of the coefficients matrix of these equations must be set equal to zero:

$$\begin{vmatrix} a_{11} & a_{12} & a_{13} \\ a_{21} & a_{22} & a_{23} \\ a_{31} & a_{32} & a_{33} \end{vmatrix} = 0 \tag{32}$$

By solving Eq. (32), the buckling load is obtained as a function of m and n. The critical buckling load is the minimum load achieved through different values of m and n.

3 NUMERICAL MODELING

A spherical shell of radius R=1 and meridional angle $\varphi_L = 30^\circ$ and circumferential angle of 360 degrees with the mechanical properties as what is given in Table 1., was simulated in Abaqus software.

The shell thickness is considered as 0.0005, the loading as hydrostatic type and the boundary conditions as simply supported. The grain size was assigned as 0.03 and Medial axis and Quad dominated type of mesh were applied. A view of the loaded shell can be seen in Fig. 3. The solution was defined as static and buckling and the problem was solved. The first buckling mode of the FGM spherical shell with the parameter $h/R = 0.003$ obtained by Abaqus simulation is shown in Fig. 4.

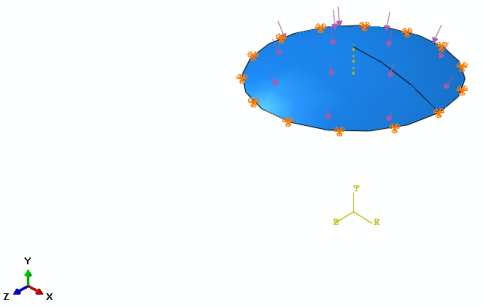

Fig.3
A view of the simply supported spherical shell subjected to hydrostatic pressure.

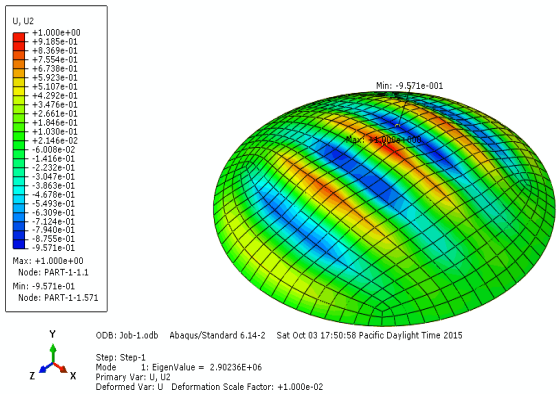

Fig.4
The first buckling mode of the FGM spherical shell with parameter $h/R = 0.003$.

Table 1
The elastic modulus of a type of steel and ceramics.

Ceramics (elastic modulus)(GPa)	Steel (elastic modulus)(GPa)
361.3	202.97

4 RESULTS AND DISCUSSION

In this section, firstly, the critical buckling pressure of the steel spherical shells is determined. After that, the classical buckling load of steel and FGM spherical shells for different values of the parameters such as dimensionless parameter h/R is attained. Then, the dimensionless critical buckling pressure versus dimensionless parameter h/R for isotropic (steel) shallow spherical shells with different values of φ_L is determined. Finally, the numerical modeling of the problem is examined using Abaqus software and the numerical results are compared with the analytical results.

Poisson's ratio of steel and ceramics are assumed to be 0.3. Simply supported boundary conditions are considered for the shell. In the graphs, the results of the hydrostatic buckling pressure are presented.

It should be noted that the classical buckling pressure of a shallow spherical shell is given in Ref. [17] as:

$$P_{cl} = \frac{2E}{\sqrt{3\left(1-\upsilon^2\right)}}\left(\frac{h}{R}\right)^2 \tag{33}$$

This parameter is used to nondimensionalize some results of the present paper.

In Fig. 5 is compared the results of the present research with the results of reference [8] for the shallow spherical shells made of pure isotropic material (metal) for which $E = E_m$. In this figure is depicted the dimensionless critical hydrostatic pressure versus the dimensionless parameter h/R for different values of φ_L. As it can be observed, there are good agreements between the results. Also, it is concluded that the classical buckling hydrostatic pressure given by expression (33), has more reliability for the larger values of φ_L. The most accurate value is for the complete spherical shell.

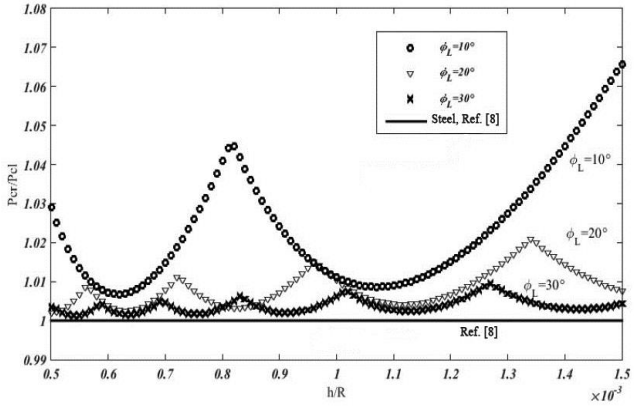

Fig.5
The dimensionless critical hydrostatic pressure versus the dimensionless parameter h/R for isotropic (steel) shallow spherical shells with different values of φ_L.

The critical hydrostatic pressure versus the dimensionless parameter h/R for steel shallow spherical shells with $\varphi_L = 30^\circ, \varphi_L = 20^\circ, \varphi_L = 10^\circ$ is shown in Fig. 6. It is seen that, by increasing the values of φ_L, the values of the present results and those of Ref. [8] become closer.

In order to further validate the soundness of the presented analytical modeling, the analytical results are compared with the results obtained numerically by Abaqus simulation. In Fig. 7 are shown the hydrostatic buckling pressure versus the dimensionless parameter h/R curves obtained by the analytical method and Abaqus simulation for spherical FG shells with k=2, E_m=202.97e9 *Pa* and E_c=361.3e9 *Pa*. As it can be observed, there is an excellent agreement between the results which confirms the validity and the accuracy of the presented analysis.

In Fig. 8 is shown the dimensionless critical hydrostatic pressure versus the dimensionless parameter h/R for the shallow spherical shells with $\varphi_L = 10^\circ$ made of steel, ceramic, and FG material for different values of the power law indices k. It is observed that by increasing the power law index, the critical hydrostatic pressure decreases. The dimensionless critical hydrostatic pressure of the FGM spherical shells is larger than that of the steel ones but it is less than that of the ceramic ones.

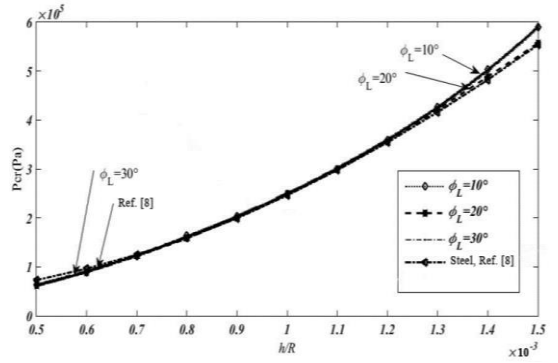

Fig.6
The dimensionless critical hydrostatic pressure versus the dimensionless parameter h/R for isotropic (steel) shallow spherical shells with different values of φ_L.

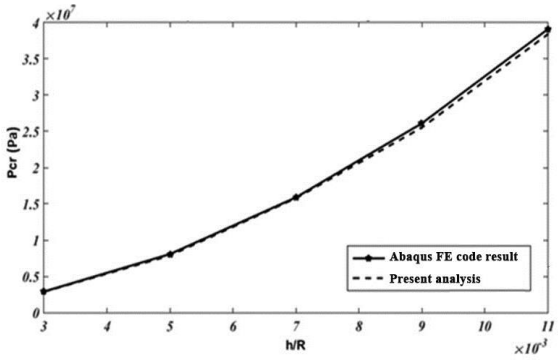

Fig.7
The hydrostatic buckling pressure of FGM spherical shells versus the dimensionless parameter h/R.

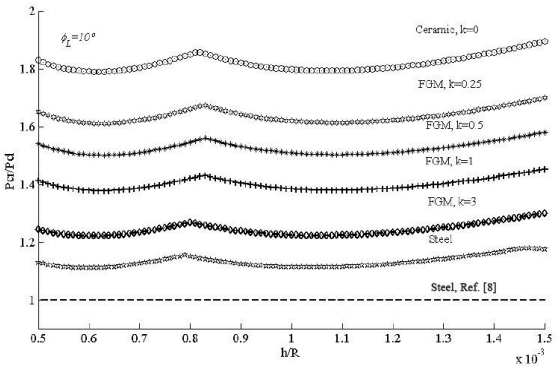

Fig.8
The dimensionless critical hydrostatic pressure versus the dimensionless parameter h/R for the steel, the ceramic, and the FGM shallow spherical shells with different power law indices *k*.

The dimensionless critical hydrostatic pressure versus the dimensionless parameter h/R for FGM shallow spherical shells with k=2 and different values of φ_L is shown in Fig. 9. According to this figure, it is concluded that for FGM shallow spherical shells, the values of the critical hydrostatic pressure and the classical one become closer for the larger value of φ_L.

In Fig. 10 is presented the dimensionless critical hydrostatic pressure of FGM shallow spherical shells versus the dimensionless parameter h/R for different values of the power law index k. As this figure show, by increasing the value of the dimensionless parameter h/R, the dimensionless critical hydrostatic pressure is almost increased. As Fig. 10 shows, the dimensionless critical hydrostatic pressure of FGM spherical shells is less than that of ceramic ones and is larger than that of steel ones. Moreover, it is seen that as the power law index k increases, the dimensionless critical hydrostatic pressure decreases.

The hydrostatic buckling pressure of FGM spherical shells versus the dimensionless parameter h/R for the values of $\varphi_L = 10^\circ, 20^\circ, 30^\circ$ and k=2 is presented in Fig. 11. As it is seen, the increase of the dimensionless parameter h/R, results in the increase of the hydrostatic buckling pressure.

In Fig. 12 is shown the hydrostatic buckling pressure of FGM spherical shells versus the power law index *k* for different values of the dimensionless parameter h/R . As it is observed, by increasing the power law index *k*, the hydrostatic buckling pressure considerably decreases from *k*=0 to *k*=1 and after that it decreases slightly. Also, at a specific value of the power law index *k*, the hydrostatic pressure increases as the dimensionless parameter h/R increases.

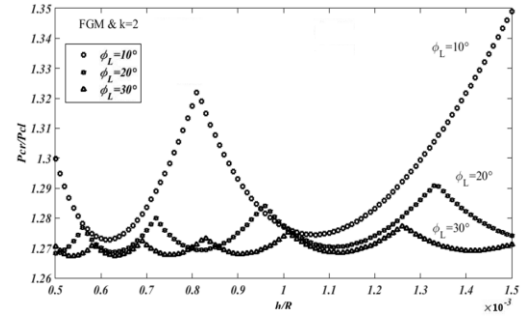

Fig.9
The dimensionless critical hydrostatic pressure versus the dimensionless parameter h/R for FGM shallow spherical shells with different values of φ_L.

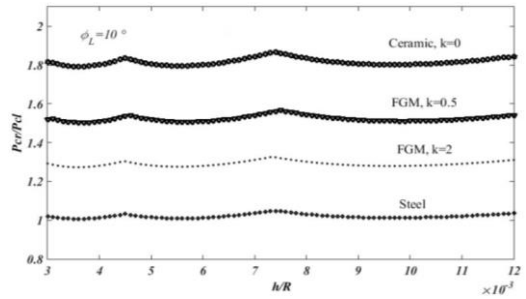

Fig.10
The dimensionless critical hydrostatic pressure of FGM shallow spherical shells versus the dimensionless parameter h/R for different values of the power law indices *k*.

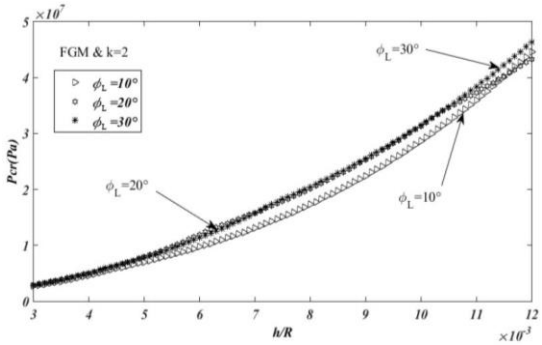

Fig.11
The hydrostatic buckling pressure of FGM spherical shells versus the dimensionless parameter h/R for different values of φ_L.

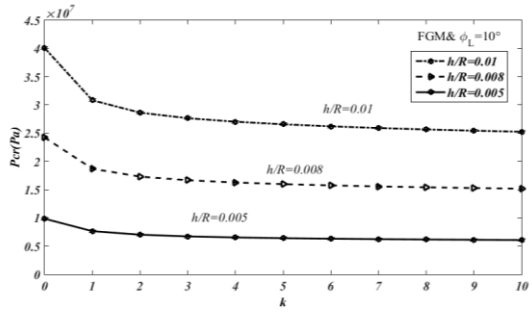

Fig.12
The hydrostatic buckling pressure of FGM spherical shells versus the power law index k for different values of the dimensionless parameter h/R .

In Fig. 13 is presented the hydrostatic buckling pressure of FGM spherical shells with *k*=2 and $h/R = 0.005$ versus the parameter E_{cm} for different values of φ_L . As it is seen, by increasing the parameter E_{cm} , the hydrostatic buckling pressure of FGM spherical shells increases. Also, by increasing the values of φ_L , the hydrostatic buckling

pressure decreases so that their values become close to each other. In Fig. 13, the parameter E_m is kept constant as $E_m = 200e9Pa$ but the value of E_c varies from 250*e*9 *Pa* to 450*e*9 *Pa*, increasing a value of 50*e*9 *Pa* in each step.

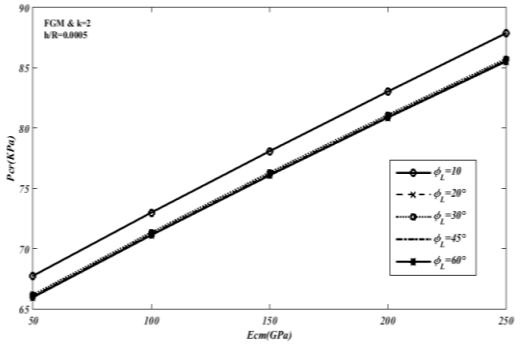

Fig.13
The hydrostatic buckling pressure of FGM spherical shells versus the parameter E_{cm}.

5 CONCLUSIONS

In this paper, the buckling analysis of simply-supported shallow FGM spherical shells subjected to hydrostatic loading is carried out. The equilibrium and stability equations of FGM shallow spherical shells are obtained. Derivations are based on the first-order shell theory of Love and Kirchhoff, the Donnell-Mushtari-Vlasov (DMV) kinematic equations and Hooke's Law. The following main conclusions are drawn:

1. Increasing the power law index *k*, causes the critical hydrostatic pressure to decrease.
2. The dimensionless critical hydrostatic pressure of FGM shallow spherical shells is less than that of ceramic ones and is larger than that of steel ones.
3. Increasing the dimensionless parameter h/R, results in the increase of the hydrostatic buckling pressure.
4. As the parameter E_{cm} increases, the hydrostatic buckling pressure of FGM spherical shells is increased.

REFERENCES

[1] Darvizeh M., Darvizeh A., Shaterzadeh A. R., Ansari R., 2010, Thermal buckling of spherical shells with cut-out, *Journal of Thermal Stresses* **33**(5): 441-458.

[2] Von Karman Th., Tsien H. S., 1939, The buckling of spherical shells by external pressure, *Journal of the Aeronautical Sciences* **7**(2): 43-50.

[3] Zang Y.Q., Zhang D., Zhou H.Y., Ma H.Z., Wang T.K., 2000, Non-linear dynamic buckling of laminated composite shallow spherical shells, *Composites Science and Technology* **60**(12-13): 2361-2363.

[4] Nie G.H., 2001, Asymptotic buckling analysis of imperfect shallow spherical shells on non-linear elastic foundation, *International Journal of Mechanical Sciences* **43**(2): 543-555.

[5] Li Q.S., Liu J., Tang J., 2003, Buckling of shallow spherical shells including the effects of transverse shear deformation, *International Journal of Mechanical Sciences* **45**(9): 1519-1529.

[6] Gupta N.K., Mohamed Sheriff N., Velmurugan R., 2008, Experimental and theoretical studies on buckling of thin spherical shells under axial loads, *International Journal of Mechanical Sciences* **50**(3): 422-432.

[7] Sørensen K.D., Jensen H.M., 2008, Buckling-driven delamination in layered spherical shells, *Journal of the Mechanics and Physics of Solids* **56**(1): 230-240.

[8] Hutchinson J.W., 2010, Knockdown factors for buckling of cylindrical and spherical shells subject to reduced biaxial membrane stress, *International Journal of Solids and Structures* **47**(10): 1443-1448.

[9] Wahhaj Uddin M., 1987, Buckling of general spherical shells under external pressure, *International Journal of Mechanical Sciences* **29**(7): 469-481.

[10] Shaterzadeh A. R., Darvizeh M., Darvizeh A., Ansari R., 2011, Thermal post-buckling of shells of revolution, *Journal of Thermal Stresses* **34**(10): 1035-1053.

[11] Sato M., Wadee M.A., Iiboshi K., Sekizawa T., Shima H., 2012, Buckling patterns of complete spherical shells filled with an elastic medium under external pressure, *International Journal of Mechanical Sciences* **59**(1): 22-30.

[12] Sabzikar Boroujerdy M., Eslami M.R., 2014, Axisymmetric snap-through behavior of Piezo-FGM shallow clamped spherical shells under thermo-electro-mechanical loading, *International Journal of Pressure Vessels and Piping* **120-121**: 19-26.
[13] Zhu Y., Wang F., Liu R., 2017, Nonlinear stability of sensor elastic element—corrugated shallow spherical shell in coupled multi-field, *Applied Mathematics and Mechanics* **38**(6): 877-888.
[14] Mirzavand B., Eslami M.R., 2007, Thermal buckling of simply supported piezoelectric FGM cylindrical shells, *Journal of Thermal Stresses* **30**(11): 1117-1135.
[15] Wunderlich W., Albertin U., 2002, Buckling behaviour of imperfect spherical shells, *International Journal of Non-Linear Mechanics* **37**(4-5): 589-604.
[16] Menaa M., Lakis A. A., 2014, Supersonic flutter of a spherical shell partially filled with fluid, *American Journal of Computational Mathematics* **4**: 153-182.
[17] Hutchinson J.W., 1967, Imperfection sensitivity of externally pressurized spherical shells, *Journal of Applied Mechanics* **34**: 49-55.
[18] Nie G.H., 2003, On the buckling of imperfect squarely-reticulated shallow spherical shells supported by elastic media, *Thin-Walled Structures* **41**(1): 1-13.